7142–7154 Nucleic Acids Research, 2010, Vol. 38, No. 20 Published online 22 June 2010
doi:10.1093/nar/gkq560

DNA synapsis through transient tetramerization triggers cleavage by Ecl18kI restriction enzyme

Mindaugas Zaremba[1], Amelia Owsicka[1], Gintautas Tamulaitis[1], Giedrius Sasnauskas[1], Luda S. Shlyakhtenko[2], Alexander Y. Lushnikov[2], Yuri L. Lyubchenko[2], Niels Laurens[3], Bram van den Broek[3], Gijs J. L. Wuite[3] and Virginijus Siksnys[1,*]

[1]Institute of Biotechnology, Graiciuno 8, LT-02241, Vilnius, Lithuania, [2]Department of Pharmaceutical Sciences, College of Pharmacy, COP 1012, University of Nebraska Medical Center, 986025 Nebraska Medical Center, Omaha, NE 68198-6025, USA and [3]Department of Physics and Astronomy and Laser Centre, VU University, De Boelelaan 1081, 1081 HV, Amsterdam, The Netherlands

Received May 5, 2010; Revised May 31, 2010; Accepted June 1, 2010

ABSTRACT

To cut DNA at their target sites, restriction enzymes assemble into different oligomeric structures. The Ecl18kI endonuclease in the crystal is arranged as a tetramer made of two dimers each bound to a DNA copy. However, free in solution Ecl18kI is a dimer. To find out whether the Ecl18kI dimer or tetramer represents the functionally important assembly, we generated mutants aimed at disrupting the putative dimer–dimer interface and analysed the functional properties of Ecl18kI and mutant variants. We show by atomic force microscopy that on two-site DNA, Ecl18kI loops out an intervening DNA fragment and forms a tetramer. Using the tethered particle motion technique, we demonstrate that in solution DNA looping is highly dynamic and involves a transient interaction between the two DNA-bound dimers. Furthermore, we show that Ecl18kI cleaves DNA in the synaptic complex much faster than when acting on a single recognition site. Contrary to Ecl18kI, the tetramerization interface mutant R174A binds DNA as a dimer, shows no DNA looping and is virtually inactive. We conclude that Ecl18kI follows the association model for the synaptic complex assembly in which it binds to the target site as a dimer and then associates into a transient tetrameric form to accomplish the cleavage reaction.

INTRODUCTION

Restriction endonucleases (REases) are found in most of bacteria and archaea and provide a defence barrier against invasion by foreign (e.g. bacteriophage) DNA. They come in a wide variety of types and subgroups. Type II REases recognize short DNA sequences usually 4–8 bp in length and cut both DNA strands within or close to their target sites to generate a double strand break (1). To provide protection against invading DNA, REases must discriminate between alien and host DNA. The identity tags are provided by accompanying DNA methyltransferases which transfer a methyl group to the A or C bases within the REase target site and render host DNA resistant against REase cleavage. Therefore, an extreme fidelity in target site recognition and tight coupling between sequence recognition and catalysis are crucial for the biological function of restriction enzymes. To ensure faithful target site recognition and cleavage, REases adopt diverse mechanistic strategies.

Most of REases belong to the PD...EXK family and share a conserved structural scaffold, which harbours the active site residues involved in coordination of the metal ion and catalysis (1,2). Typically, REases of the PD... EXK family contain a single active site per monomer. To achieve cleavage of both DNA strands, restriction enzymes assemble into different oligomeric structures and follow different mechanisms. For example, MvaI and BcnI (3,4) function as monomers and use a single active site to introduce a double-strand break by nicking separate DNA strands. PLD family nuclease BfiI, which

*To whom correspondence should be addressed. Tel: +370 5 2602108; Fax: +370 5 2602116; Email: siksnys@ibt.lt
Present address:
Bram van den Broek, Physics of Life Processes, Leiden Institute of Physics, Leiden University, Niels Bohrweg 2, 2333 CA Leiden, The Netherlands.

The authors wish it to be known that, in their opinion, the first two authors should be regarded as joint First Authors.

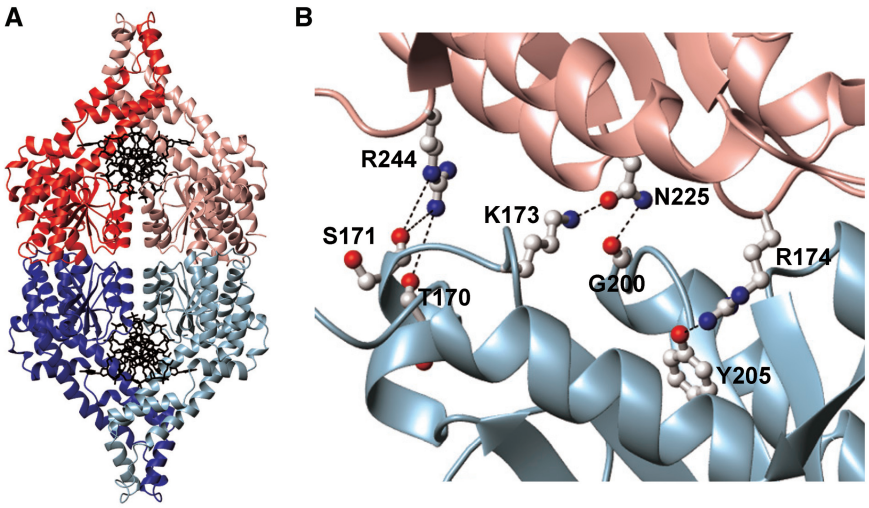

Figure 1. Crystal structure and tetramerization interface of Ecl18kI REase. (**A**) Ribbon representation of the two primary dimers of Ecl18kI (blue and red, respectively) bound to two copies of cognate DNA (black). (**B**) Close-up view of the Ecl18kI tetramerization interface showing the contacts of the residues R174, N225 and R244, which were subjected to mutagenesis.

is a dimer but contains a single active site, follows a similar strategy (5). Orthodox PD...EXK family REases such as EcoRI or BamHI are homodimers and each monomer contains a single active site, which acts on a separate DNA strand to generate a double-strand break (6). Yet another subgroup of REases function as tetramers with the two primary dimers resembling the orthodox enzymes (7). Such tetrameric REases bind two target DNA copies and generate double-strand breaks at both sites cutting four phosphodiester bonds simultaneously (8–11). Tetramerization provides stabilization of the functional REase dimer (12,13) and increase the specificity of target site recognition (14). A few REases assemble into transient oligomeric intermediates to achieve DNA double-strand breaks. An archetypal FokI REase is a monomer in solution but dimerizes upon DNA binding to cut both DNA strands (15,16). The monomeric Eco29kI nuclease of the GYI-YIG family also forms a transient dimer for DNA cleavage (17). Surprisingly, the Cfr42I endonuclease, which acts on the same DNA sequence and shares sequence similarities with Eco29kI, is a stable tetramer (18). On the other hand, the PD...EXK family nuclease SgrAI is a dimer in solution but for DNA cleavage assembles into a transient tetramer through the association of two DNA-bound dimers (19,20).

The Ecl18kI restriction enzyme recognizes an interrupted pentanucleotide sequence 5′-CCNGG-3′ (where N stands for any nucleotide) and cleaves it before the first C in both strands to generate a double-strand break (21). Ecl18kI (22) is a founding member of a REase family (23,24), which flips nucleotides within the recognition sequence to achieve specificity and enable DNA cleavage. Surprisingly, according to the crystal structures, the nucleotide flipping REases associate into different oligomeric structures. PspGI and EcoRII-C, specific for the CCWGG sequence (where W stands for A or T), are arranged as dimers both in the crystal and in solution (23–27). However, the crystal structure of Ecl18kI solved in the DNA-bound form (22), shows a tetramer arranged of two primary dimers each bound to a single DNA site (Figure 1A). A primary Ecl18kI dimer reveals a remarkable structural similarity to the PspGI REase dimer (23). Moreover, analytical ultracentrifugation experiments demonstrate that Ecl18kI in the DNA-free form is a dimer in solution (28). This raises the question of whether the tetramer (Figure 1A) is a crystal packing artefact or represents a functionally important oligomeric form of Ecl18kI.

To answer this question, we have generated Ecl18kI mutants aimed at disrupting the dimer–dimer interface seen in the crystal and analyse the functional properties of the wild–type (wt) Ecl18kI and mutant proteins using a combination of biochemical and biophysical methods. We show here by atomic force microscopy (AFM) that on DNA containing two recognition sites, the Ecl18kI tetramer synapses two sites loops out the intervening DNA. Using the tethered particle motion (TPM) technique, we demonstrate that DNA looping by Ecl18kI is highly dynamic and involves transient association of two DNA bound dimers. Furthermore, we provide experimental evidence that Ecl18kI cleaves DNA in a synaptic complex much faster than when acting on a single recognition site. In contrast to Ecl18kI, the tetramerization interface mutant R174A binds to cognate DNA as a dimer, shows no DNA looping either in AFM or TPM assays and cuts DNA very slowly.

MATERIALS AND METHODS

Oligonucleotides

Oligodeoxynucleotides for DNA binding and cleavage studies (Table 1) were purchased from Metabion (Martinsried, Germany). The DNA duplexes were assembled by mixing and annealing appropriate complementary DNA strands at equimolar ratios in the annealing

Table 1. Oligoduplexes used in this study

Oligoduplex	Sequence	Specification
bio-SP33	5′-AATGGGCTCGCACGCCTGGTATTATCGATTGTA-3′ 3′-TTACCCGAGCGTGCGGACCATAATAGCTAACAT-5′	Biotinylated 33-bp cognate oligoduplex (Ecl18kI recognition sequence underlined).
SP25	5′-CGCACGACTTCCTGGAAGAGCACGC-3′ 3′-GCGTGCTGAAGGACCTTCTCGTGCGTTG-5′	25-bp cognate oligoduplex.
SP25(PTO)	5′-CGCACGACTTsCCTGG-AAGAGCACGC-3′ 3′-GCGTGCTGAA-GGACCsTTCTCGTGCGTTG-5′	25-bp cognate oligoduplex containing phosphorothioate linkages at the scissile positions.
NSP25	5′-CGCACGACTTGTCACAAGAGCACGC-3′ 3′-GCGTGCTGAACAGTGTTCTCGTGCGTTG-5′	25-bp non-cognate oligoduplex lacking the Ecl18kI recognition site.

buffer (33 mM Tris-acetate, pH 7.9 at 25°C, 66 mM potassium acetate). The 5′-termini of DNA oligonucleotides were radiolabelled using the 'DNA labeling kit' (Fermentas, Vilnius, Lithuania) and [γ-^{33}P]ATP (Hartmann Analytic, Braunschweig, Germany).

DNA fragments

DNA fragments for AFM and DNA binding/cleavage studies were obtained by a polymerase chain reaction (PCR) amplification of selected regions of the pTZ19R plasmid and purified as described (29–31). AFM studies employed the 445-bp PCR fragment containing a single copy of the Ecl18kI recognition site 5′-CCNGG-3′ and the 493-bp PCR fragment containing two Ecl18kI sites. For DNA binding and kinetic studies the one- and two-site fragments were radiolabelled by adding [α-^{33}P]dATP (Hartmann Analytic, Braunschweig, Germany) to PCR reactions. One- and two-site DNA fragments for TPM experiments were synthesized by PCR using plasmids pEcoRII-1 and pEcoRII-3 as a template (32). Primers used for PCR contained biotin or digoxigenin at the 5′-end resulting in the DNA fragments labelled with biotin on one end and digoxigenin on the other. Both DNA fragments are 1050 bp in length. The one-site DNA fragment contains a single recognition sequence of Ecl18kI 260 bp from one end. The recognition sequences of Ecl18kI in the two-site fragment are separated by 520 bp and are located 260 bp from the ends. The concentrations of DNA fragments were determined by densitometric analysis of samples separated on 1.5% agarose gels in the electrophoresis buffer [100 mM H_3BO_3–NaOH, pH 8.2, 15 mM sodium acetate, 2 mM ethylenediaminetetraacetic acid (EDTA) and 0.5 μg ml^{-1} ethidium bromide].

Proteins

The wt Ecl18kI and R174A, N225A and R244A variants of Ecl18kI were purified as described earlier (33). Protein concentrations were determined by measuring absorbance at 280 nm. The extinction coefficient for Ecl18kI dimer (77660 M^{-1} cm^{-1}) was calculated using the 'ProtParam' tool (http://www.expasy.ch/).

Mutagenesis

The R174A, N225A and R244A mutants of Ecl18kI were obtained similarly to (33). Sequencing of the entire gene of each mutant confirmed that only the designed mutation had been introduced. The specific cleavage activity of the Ecl18kI mutants was determined using phage lambda DNA as described (27).

Gel mobility shift assay

^{33}P-labelled oligoduplexes (0.2 nM) or DNA fragments (0.3 nM) were mixed with increasing amounts of protein in the binding buffer [40 mM Tris–acetate, pH 8.3 at 25°C, 5 mM calcium acetate, 0.1 mg ml^{-1} bovine serum albumin (BSA), 10 % v/v glycerol], incubated for 10 min at room temperature and reaction mixtures were analysed on the non-denaturing 6 or 8% polyacrylamide gel (ratio of acrylamide/*N*,*N*′-methylenebisacrylamide 29:1) using 40 mM Tris-acetate (pH 8.3 at 25°C) supplemented with 5 mM calcium acetate as the running buffer. Electrophoresis was run at room temperature for 3–5 h at ~6 V cm^{-1}.

AFM experiments

The complexes of Ecl18kI protein with 493-bp DNA fragment were prepared in binding buffer as described above at several protein/DNA ratios. After formation of the complex the reaction mixture was incubated at room temperature for 10 min in the presence of 0.5% glutaraldehyde (GA). The fixation reaction was stopped by adding 2 M Tris–HCl (pH 7.4 at 25°C). Appropriate dilutions were made before deposition of the samples onto mica in order to provide an even spread of DNA on the surface for AFM imaging.

Functionalized mica (APS-mica) was used as AFM substrate [see details in (34–37)]. Briefly, DNA samples (5 µl) were deposited on APS-mica for 2 min, washed with deionized water (Aquamax Lab. Water System) and dried with Ar gas. The images were collected on NanoScope IV system (Veeco/Digital Instruments, Santa Barbara, CA, USA) operating in tapping mode in air. Tapping Mode Etched Silicon Probes (TESP; Veeco/Digital Instruments, Inc.) with a spring constant of 42 N m^{-1} and a resonant frequency between 270–320 kHz were used. The scan rate was 1.7 Hz.

AFM data analysis

To confirm the specificity of the Ecl18kI–DNA complexes, the position of the protein in each type of the complex was calculated based on DNA contour length and the theoretical lengths of the DNA arms. The volume of the protein

was estimated from the measured height and diameter of the protein blob as described earlier (29,37). The volume of the protein was converted into mass in kilodaltons dividing by an appropriate conversion coefficient [see details in (30,37,38)]. Femtoscan Online software (Advanced Technologies Center, Moscow, Russia) was used to trace the DNA contour length and to measure the height and diameter of the protein. The histograms for protein position and volume measurements were analysed using Origin 6.0 software (Originlab, Northampton, MA, USA) and fitted by Gaussian curves to determine the most probable values for the Ecl18kI position and volume.

TPM experiments

Dynamic looping of the Ecl18kI enzyme was studied in real time using a TPM setup. In our assay we tethered DNA molecules between the glass surface of a flow cell and a 440-nm polystyrene bead (39). Changes in the DNA length, for example, by protein-induced DNA looping, were detected by measuring the distribution [i.e. the root mean square (RMS)] of the Brownian motion of the bead in time. All measurements were performed using an inverted microscope (Nikon TE 2000 Eclipse). Sample preparation, data acquisition and tether selection were done as described previously (39). Several different TPM experiments were conducted using a single flow cell containing tens of single DNA tethers in a buffer containing 33 mM Tris–acetate, pH 7.9 at 25°C, 66 mM potassium acetate, 2 mM $CaCl_2$ and 0.15 mg ml^{-1} α-casein.

TPM data analysis

The TPM data were analysed by fitting a double Gaussian function to the RMS histograms to obtain a threshold value to separate the looped and the unlooped states. This established method works well when both states are clearly separated (40). However, since the looped state for the wt Ecl18kI is short lived (~1 s, see 'Results' section) multiple looping events are needed in order for the looped state to be distinguishable from the unlooped state in the RMS histogram. A well-defined threshold value is found for Ecl18kI concentrations of 3 nM and higher, but in fact, at Ecl18kI concentration <3 nM the small number of looping events makes it impossible to fit reliably a second Gaussian and hence find a threshold value.

To solve this problem we performed experiments at different protein concentrations without changing the flow cell. This enabled us to study the behaviour of individual DNA molecules as a function of Ecl18kI concentration, eliminating heterogeneity between DNA and samples. For all protein concentrations each tether was individually analysed. Using the threshold value found at high protein concentration (≥3 nM) enabled us to detect looping events at low Ecl18kI concentrations without fitting two Gaussians to the RMS histograms. The looping and unlooping rates were obtained by fitting the dwell times to a three-state model as described in (39). Kinetic data, however, suggest that the reaction pathway of Ecl18kI has four states (Figure 7B).

The simplification to a three-state model does not impact on the looping and unlooping rates, but it does prohibit calculating the proper association and dissociation rates. These rates are instead obtained from the equilibrium distribution of the dwell times. This distribution is the ratio of the areas under the two fitted Gaussians. Predicted equilibrium distributions as a function of association and off rate were obtained using reaction pathway simulations written in the analysis software Berkeley Madonna. Our measured distribution was subsequently fitted to these simulations to obtain the protein dissociation rate. The simulations also revealed that at protein concentrations >3 nM, the four-state model collapses to the three state model permitting the direct calculation of the protein association rate.

Reactions with oligonucleotide duplexes

The cleavage reactions on the immobilized oligoduplex bio-SP33 radiolabelled on the bottom DNA strand were performed at 20°C in the reaction buffer (33 mM Tris-acetate, pH 7.9 at 25°C, 66 mM potassium acetate, 10 mM magnesium acetate and 0.1 mg ml^{-1} BSA). Immobilization of the oligonucleotide on streptavidin-coated beads was performed as described (5,12). The final concentrations of immobilized oligoduplex and enzyme dimer were ~1 and 1000 nM respectively. In parallel, the immobilized oligoduplex cleavage reactions were performed in the presence of 500 nM of non-biotinylated cognate SP25(PTO), non-cognate NSP25 or precleaved cognate SP25 DNA duplexes (Table 1) in solution. In a separate set of experiments, the non-immobilized radiolabelled bio-SP33 substrate (1 nM) was cleaved by 1000 nM of enzyme in the presence of 500 nM of the SP25(PTO) oligoduplex. Aliquots were removed at timed intervals and quenched with phenol/chloroform. The aqueous phase was mixed with loading dye [95% (v/v) formamide, 20 mM EDTA and 0.01% (w/v) bromphenol blue] before denaturing gel electrophoresis. The 20% (w/v) polyacrylamide gels (29:1, acrylamide/*N*,*N*′-methylenebisacrylamide) in Tris–borate containing 8.5 M urea were run at 30 V cm^{-1}. Radiolabelled DNA was detected and quantified by Cyclone Phosphor-Imager (Perkin-Elmer, Wellesley, MA, USA). The DNA cleavage rate constants were determined by fitting single exponentials to the substrate depletion data. Non-linear regression analysis employed the KYPLOT 2.0 software (41).

Reactions with DNA fragments

The cleavage reactions of one- and two-site DNA fragments used in AFM experiments were performed at 37°C in the low and high ionic strength reaction buffers. The low ionic strength (130 mM) buffer was identical to the reaction buffer described above; the high ionic strength (230 mM) buffer was prepared by addition of 100 mM potassium acetate to the low ionic strength buffer. The final concentrations of DNA and enzyme in the reaction mixture were 1 nM and 2 nM (dimer), respectively. Aliquots were removed at timed intervals and quenched with loading dye solution [75 mM EDTA, pH

8.0, 0.01% bromphenol blue, 0.3% sodium dodecyl sulphate (SDS) and 50% (v/v) glycerol]. The non-denaturing 6% (w/v) polyacrylamide gels (29:1, acrylamide/*N*,*N*′-methylenebisacrylamide) in 40 mM Tris–acetate and 1 mM EDTA were run at 7.5 V cm^{-1}. Radiolabelled DNA was detected and quantified as described above. Rate constants of DNA cleavage were determined by fitting single exponentials to the substrate depletion data.

RESULTS

Tetramerization interface mutants

In the crystal structure of the Ecl18kI-DNA complex, two DNA-bound Ecl18kI dimers are sitting back-to-back to each other making a tetramer (22) (Figure 1A). Nearly 3400 Å^2 of the accessible surface area is buried at the dimer–dimer interface. A similar surface is hidden at the tetramerization interface in the *bona fide* tetrameric REases Cfr10I and Bse634I (10,11). However, in contrast to Cfr10I and Bse634I, where non-polar hydrophobic interactions contribute to the tetramer assembly, polar interactions dominate at the Ecl18kI dimer–dimer interface. In the Ecl18kI crystal structure, R174, N225 and R244 residues make an intricate network of interactions at the dimer–dimer interface (Figure 1B), but do not contribute directly to the assembly of an individual dimer. Therefore, we assumed that these residues support the structural integrity of the Ecl18kI tetramer, but may have no effect on the Ecl18kI dimer. To probe the role of the R174, N225 and R244 residues in the Ecl18kI function, alanine replacement mutants were generated by site-directed mutagenesis. Mutant proteins were expressed in *Escherichia coli* and purified to >95% homogeneity.

DNA binding and cleavage by the R174A, N225A and R244A mutants

DNA binding was analysed by gel mobility shift assay using two different 25-bp oligoduplexes. The cognate SP25 oligoduplex contained the Ecl18kI recognition sequence, while the non-specific NSP25 oligoduplex lacked the target site (Table 1). Experiments were performed in the presence of Ca^{2+} ions, which do not support the Ecl18kI catalysis but are necessary for the specific DNA binding (28). Gel shift experiments were quantified and K_d values determined as described (28). Binding data indicate that the alanine replacement of residues R174, N225 and R244 have little effect both on cognate (Table 2) and non-cognate oligoduplex binding (data not shown).

In contrast to the minor changes in the cognate DNA binding affinity, λ DNA cleavage activity of the N225A and R174A mutants is severely compromised. Indeed, the N225A and R174A mutants display, respectively, 100- and 500-fold reduced λ DNA cleavage activity compared with the wt Ecl18kI (Table 2). The R224A mutation has little effect both on cognate DNA binding and λ DNA cleavage. Hence, a preliminary biochemical analysis suggests that the N225A and R174A mutations at the Ecl18kI tetramerization interface significantly impair DNA cleavage but have only a small effect on DNA binding. To understand the effect of mutations at the tetramerization interface on the Ecl18kI function, the catalytically deficient R174A mutant was subjected to detailed analysis.

Table 2. Cognate DNA binding (K_d) and phage λ DNA cleavage activity of wt Ecl18kI and mutant variants

Protein	K_d, nM	Cleavage activity, %
Wt	0.2 ± 0.1	100
R174A	1.1 ± 0.1	0.2
N225A	0.8 ± 0.1	1
R244A	1.3 ± 0.3	14

The two-site DNA binding pattern is different for the wt Ecl18kI and the R174A mutant

If the Ecl18kI tetramer is a functional unit in solution it may interact with two DNA sites simultaneously. On the other hand, the dimeric Ecl18kI variant is able to bind only a single copy of cognate DNA. *Bone fide* tetrameric REases such as SfiI show different binding patterns on single- and two-site DNA (42). Therefore, we have studied Ecl18kI and R174A mutant binding using 445 and 493-bp DNA fragments which contain a single or two target sites, respectively.

The binding patterns of the wt Ecl18kI and the R174A mutant on the one-site 445-bp DNA fragment are nearly identical (Figure 2, top panels) and show discrete shifted bands with an identical mobility at low protein concentrations. These bands are absent in the case of the non-specific DNA fragment, which lacks the recognition site (data not shown). On the other hand, at increased protein concentrations, discrete shifted bands are transformed into smears similar to the ones observed for the non-specific DNA fragment (data not shown). Thus, single-site DNA binding patterns suggest that the wt Ecl18kI and the R174A mutant have the same DNA binding stoichiometry and binding affinity.

In the next step, the DNA binding by wt Ecl18kI and R174A mutant was examined using the 493-bp DNA fragment containing two recognition sites (Figure 2, bottom panel). At low protein concentrations, both proteins bind the two-site DNA with similar affinity to generate discrete shifted bands with identical mobility. However, the wt Ecl18kI and R174A mutant binding patterns diverge with increasing protein concentrations. The wt Ecl18kI >1 nM concentration yields a band that hardly enters the gel. On the other hand, the R174A mutant yields a second well-defined discrete band (Figure 2, bottom right panel), which shows intermediate mobility in respect to the R174A mutant at low concentration and the wt Ecl18kI at high protein concentration.

Ecl18kI is a dimer in solution but shows a tetramer bound to the two DNA molecules in the crystal. If the Ecl18kI dimer is functionally active (e.g. is able to locate and bind to the target site), on the two-site DNA, Ecl18kI dimers may first bind to the separate recognition sites and then associate into a tetramer synapsing two DNA sites

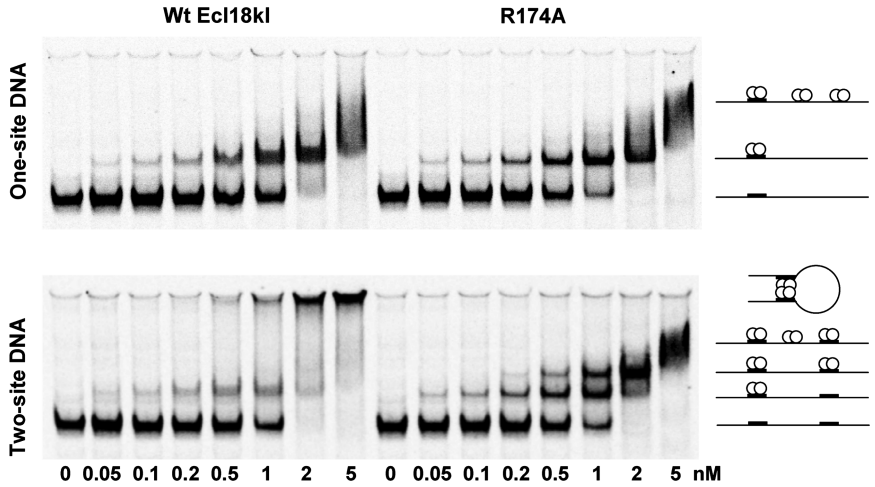

Figure 2. Binding of one- and two-site DNA by wt Ecl18kI and R174A mutant. DNA-binding was analysed by gel mobility-shift assay using 445- and 493-bp DNA fragments which contain one or two target sites, respectively. The reactions contained 0.3 nM of the ^{33}P-labelled DNA, and the protein at concentrations (in terms of nM dimer) as indicated below each lane. After 10 min incubation at room temperature, the samples were subjected to PAGE for 5 h and analysed as described in 'Materials and Methods' section. The cartoons illustrate the protein–DNA complexes presumed to correspond to each band.

located *in cis* and looping out an intervening DNA sequence. Such a model implies distinct binding patterns at different protein concentrations. At [protein] < [DNA], the Ecl18kI dimer will be bound to one of the target sites. At [protein] > [DNA], both target sites will become occupied by the individual Ecl18kI dimers which subsequently may associate into the tetramer. We suppose that the Ecl18kI binding pattern on the two-site DNA is consistent with this model. Indeed, a single discrete band is observed at [protein] < [DNA] and most likely corresponds to the Ecl18kI dimer bound to one of the target sites. The band observed at the top of the gel at [protein] > [DNA] may correspond to the looped Ecl18kI–DNA complex (Figure 2, bottom left panel). Such a binding model implies that in the case of a single-site DNA, two DNA-bound Ecl18kI dimers should associate into a tetramer containing two DNA molecules bound *in trans* (*trans*-synaptic complex). Such a complex, however, is not detected in the gel (Figure 2, top left panel). The possible explanation is that the *trans*-synaptic complex is less stable than the complex between the two DNA-bound dimers located *in cis*, and it, therefore, dissociates in the gel during the electrophoresis.

The R174A mutant differs from the wt Ecl18kI by a single mutation at the tetramerization interface. The DNA binding pattern of the R174A mutant on the single site DNA fragment is indistinguishable from that of the wt Ecl18kI (Figure 2, top panels). However, on two-site DNA, the binding patterns of the wt Ecl18kI and R174A differ at [protein] > [DNA] (Figure 2, bottom panels). If the mutation interferes with tetramer formation, the two R174A dimers presumably bind to the individual recognition sites on the same DNA molecule but fail to associate into a tetramer looping out DNA. Indeed, instead of the low mobility complex characteristic for the wt Ecl18kI on the two-site DNA at [protein] > [DNA], the R174A mutant produces two individual discrete complexes which may represent dimers bound to one and two recognition sites, respectively.

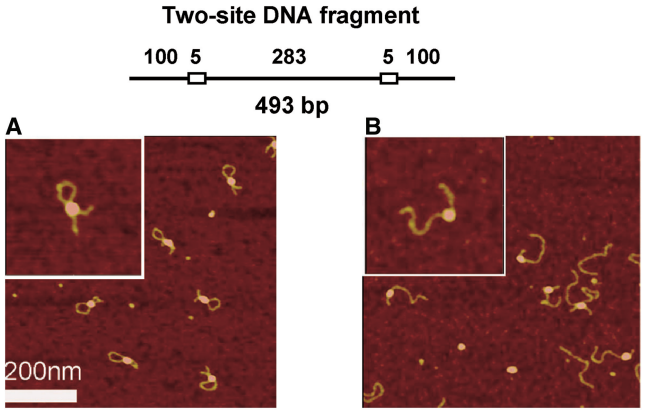

Figure 3. AFM images in air of wt Ecl18kI (**A**) and R174A mutant (**B**) complexes with two-site DNA. Image size is 700 nm. Insert in (A) is the zoomed image of a typical looped wt Ecl18kI–DNA complex (yield 67%, $N = 179$). The estimated size of the protein in a synaptic complex corresponds to the tetramer. In the case of the R174A mutant (B), the yield of the looped complexes is 3.4% ($N = 144$). The estimated size of the protein for the complex shown in the inset corresponds to a dimer.

AFM experiments show DNA looping by the wt Ecl18kI

Next, we visualized the protein-DNA complexes using the same 445- and 493-bp DNA fragments analysed in the gel-shift experiments (Figure 2). A typical AFM image of the wt Ecl18kI complex formed with the DNA fragment containing two recognition sites is shown in Figure 3A. This image shows only looped complexes, although occasionally complexes with non-looped linear DNA substrates were observed. Figure 3A clearly illustrates the formation of a looped structure [67% yield of the looped complexes among all complexes analysed ($N = 179$)] and the insert zooms in on a looped complex.

To determine whether Ecl18kI is specifically bound to the recognition sequences, we measured the length of the DNA arms in the complex and found a perfect correlation between the measured (33 ± 1 nm) and the expected value (34 nm) for the DNA arms. Using the unique capability of AFM to measure the objects in three dimensions (29–31,37,38,43,44), we determined the volume of the protein in the complex with DNA and evaluated the molecular mass of the protein. The results of such measurements (Supplementary Figure S1) for the wt Ecl18kI protein indicate a molecular mass of 145 kDa, suggesting a tetrameric stoichiometry of the protein within the looped complex (expected mass of Ecl18kI tetramer is 144 kDa). A smaller fraction of the DNA molecules are linear and contain the Ecl18kI dimer bound to a single recognition site (images not shown).

Using a single-site DNA fragment we also visualized by AFM (Supplementary Figure S2), the X-like synaptic complexes of Ecl18kI containing two DNA molecules bound *in trans*. Protein volume/molecular mass analysis in the X-like complex is consistent with a tetrameric assembly of Ecl18kI. Thus, while *in trans* Ecl18kI synaptic complexes were not detected in the gel-shift experiments, AFM studies visualized such complexes. The AFM imaging was instrumental for additional characterization of *trans*-synaptic complexes. Using single-site DNA substrates with different lengths, we were able to distinguish between homologous and heterologous complexes (row C in Supplementary Figure S2) and discriminate between the various orientations of the recognition sites within the synaptic complexes (Supplementary Figure S3) (37,44). The length measurement analysis of the AFM data led us to conclude that the DNA duplexes in the *trans*-synaptic complex are arranged in the side-by-side orientation and the enzyme forms synaptic complexes regardless of the orientation of the recognition sites.

AFM experiments performed with the R174A mutant and the two-site DNA fragment revealed two major differences between the wt Ecl18kI and the mutant variant. First, the yield of the looped structures for the R174A mutant was only 3.4% ($N = 144$) compared with 67% for the wt protein. Second, complexes with various locations of the protein on the DNA substrate appear (Figure 3B). The volume of the R174A complexes located at specific sites indicates a molecular mass of 69 kDa corresponding to the dimeric oligomeric state.

Thus, AFM studies show that the wt Ecl18kI protein bridges two recognition sites either *in cis* or *in trans* acting as a tetramer utilizing the association model for synapsis formation. The ability of Ecl18kI to form a synaptic complex is practically eliminated by the R174A mutation.

TPM experiments reveal dynamics of DNA looping in the Ecl18kI complexes

The DNA fragments used in the TPM experiments were 1050 bp in length to achieve a reliable signal change upon DNA looping. The one-site DNA fragment contained a single recognition sequence for Ecl18kI 260 bp from one end. The Ecl18kI target sites in the two-site fragment are separated by 520 bp and are located 260 bp from the ends. The RMS traces of the motion of a single DNA tether in the presence of 5 nM Ecl18kI obtained by TPM show clear signals of dynamic looping and unlooping events for the two-site DNA (Figure 4A, left panel). The histogram of a full-time trace fits well to a double Gaussian, the two levels correspond to the free DNA tether and DNA looped by Ecl18kI. Even though the DNA is looped about 16% of the total time (area of the small Gaussian), the threshold value separating the two states is clearly determined (dotted line). Above 10 nM wt Ecl18kI, the DNA appears to be condensed due to non-specific interactions because the RMS histogram smears out into smaller non-defined distributions (data not shown). Similar effects at high concentrations have been seen for various other REases (39,45). Control measurements using DNA tethers containing one recognition site show no dynamic behaviour at 5 nM, confirming the specificity of DNA looping, though at high protein concentration, DNA condensation is observed even with the one-site fragment. Interestingly, the tetramerization deficient R174A mutant, which essentially lost the ability to build loops according to AFM data, shows neither dynamic nor non-specific looping at concentrations up to 100 nM (Supplementary Figure S4A).

The dwell times for the looped and unlooped states are extracted as described in the 'Materials and Methods' section, yielding an average rate and a corresponding standard error. All rates obtained are plotted as a function of protein concentration (Figure 4B and C). The dwell times of the unlooped states are fitted to a double exponential, with the faster rate yielding a loop formation rate constant of $k_{loop} = 0.15 \pm 0.01\,s^{-1}$ (reduced χ^2: 0.8, Supplementary Figure S4B). However, the excluded volume effect of the tethered bead causes an effective stretching force of roughly 30 fN on the DNA, decreasing the actual loop formation rate by a factor of 4 (46). Hence, the corrected loop formation k_{loop} should be $\sim 0.6\,s^{-1}$. The slower rate of the double exponential fit corresponds to the protein association rate. However, at low protein concentrations the assumed three-state model does not hold (see 'Materials and Methods' section). The protein association rate constant, k_{on}, was therefore determined using the 5 nM Ecl18kI data set, resulting in a rate of $1.0 \pm 0.5 \times 10^7\,M^{-1}\,s^{-1}$ (Supplementary Figure S4B). The dwell times of the looped state yield a loop breakage rate constant $k_{unloop} = 0.86 \pm 0.03\,s^{-1}$ (reduced χ^2: 2.9, Figure 4C). The equilibrium occupancy of the looped state is plotted as a function of protein concentration in Figure 4D. The three lines (red, blue and green) were obtained from the equilibrium simulations at different off rate constants, k_{off}, using the previously determined k_{loop}, k_{on} and k_{unloop} rate constants. The data are then fitted to this model resulting in a protein dissociation rate constant (k_{off}) ranging between $0.0005\,s^{-1}$ and $0.002\,s^{-1}$ (best fit: $0.001\,s^{-1}$, reduced χ^2: 3.4).

Binding of two DNA sites by Ecl18kI promotes DNA cleavage

Bona fide tetrameric REases show optimal catalytic activity interacting with two copies of cognate DNA

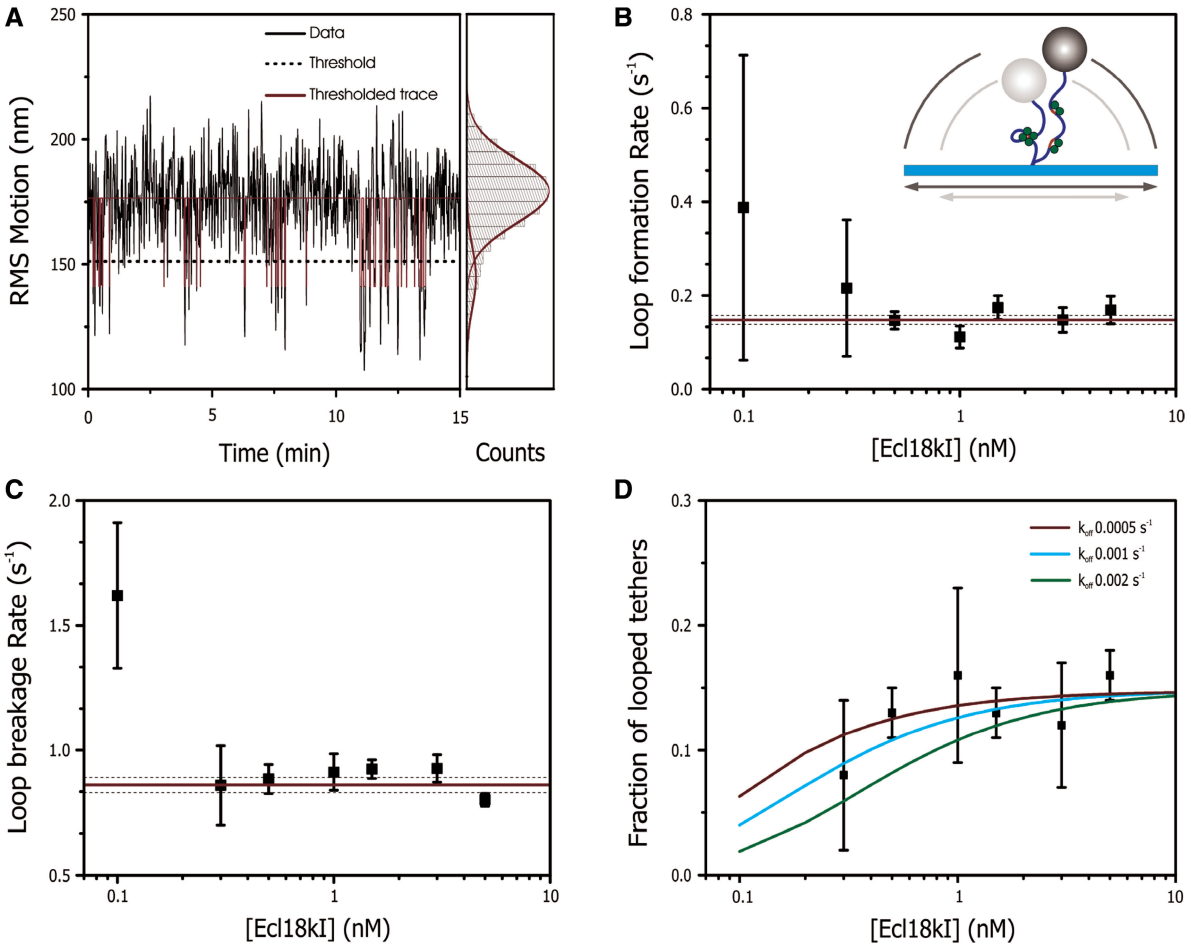

Figure 4. TPM results. (**A**) The raw RMS data are shown in the left panel (black), revealing very short-lived looped states (spikes). The dashed line shows the thresholding value used to obtain the thresholded trace (red line). In the right panel, the histogram of the RMS trace is shown. The looped and unlooped distributions fitted by a double Gauss are drawn in red. (**B**) Shown is the obtained loop formation rate along with the average value (red line) and the confidence limits (dashed lines) as given by the standard error of the average ($0.15 \pm 0.01\,s^{-1}$). The inset shows a schematic representation of the TPM assay. The dark grey to light grey semi-circles depict the reduction in bead motion from the unlooped state to the Ecl18kI-induced looped state that causes the decrease in the RMS signal. (**C**) The loop breakage rate is plotted as a function of Ecl18kI concentration. Shown in red is the averaged value, the dotted line represents the confidence limit as given by the standard error of the average ($0.86 \pm 0.03\,s^{-1}$). (**D**) Plotted is the fraction of looped tethers obtained from the equilibrium distributions between the looped and unlooped states as a function of protein concentration. Shown is the calculated curve for different protein dissociation rate constants, k_{off}, of 0.0005, 0.001 and $0.002\,s^{-1}$ (red, blue and green curves, respectively). Numerical fitting of the model to the data yielded a protein dissociation rate constant ranging between $0.0005\,s^{-1}$ and $0.002\,s^{-1}$ (best fit: $0.001\,s^{-1}$, reduced χ^2: 3.4).

and display low residual cleavage on single-site DNA (8–10,18,19,47,48). In order to determine whether Ecl18kI requires binding of two cognate DNA copies for optimal catalysis, we employed two different experimental approaches: (i) an immobilized DNA cleavage assay and (ii) a one- and two-site DNA cleavage assay in solution.

Cleavage of immobilized DNA. Immobilized DNA cleavage assay is instrumental in the studies of REases, which interact with two DNA targets (5,12,18). It minimizes enzyme interaction with two DNA molecules due to the low immobilized DNA concentration on the solid surface. In the Ecl18kI studies, a cognate oligoduplex (bio-SP33) that carries a biotin tag at the 5′-end of one strand and a radiolabel at the 5′-end of the complementary strand was used as a substrate (Table 1). The oligoduplex was immobilized on the surface of the streptavidin-coated beads at a low density (see 'Materials and Methods' section) to ensure enzyme interactions with a single cognate DNA copy. Under these conditions, simultaneous binding of two DNA molecules is excluded because neighbouring DNA molecules are located on the surface too far away from each other (Figure 5A). To evaluate the effect of the second DNA copy on the Ecl18kI cleavage, the non-labelled activator oligoduplex is added in solution (Figure 5B) enabling formation of the synaptic complex comprising a radioactively labelled immobilized oligoduplex and a non-labelled oligoduplex present in solution. Three different activators (Table 1) were used in this study: (i) a modified cognate oligoduplex SP25(PTO), which is bound but not cleaved by Ecl18kI (data not shown); (ii) a non-cognate oligoduplex NSP25, which lacks the Ecl18kI target; and (iii) a cognate oligoduplex SP25 precleaved with Ecl18kI to mimic the reaction products.

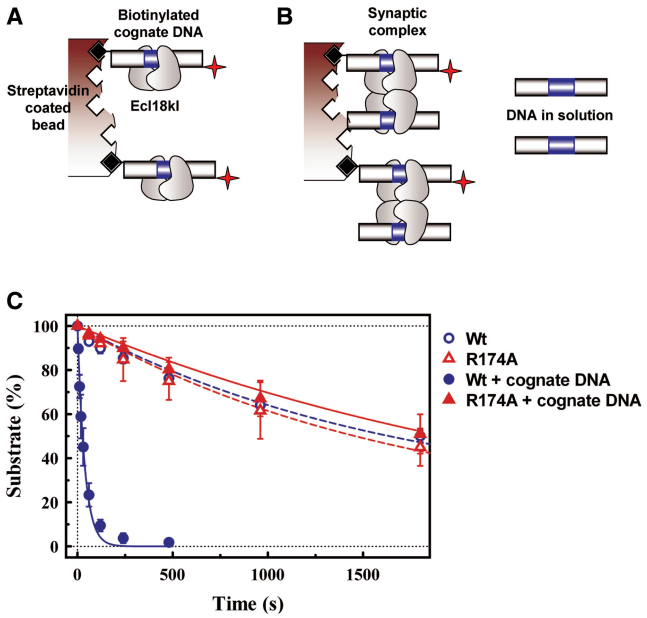

Figure 5. Immobilized DNA cleavage by Ecl18kI. Cartoons in (**A**) and (**B**) depict the experimental strategy (12). (A) Oligoduplex bio-SP33 (Table 1), which carries a biotin tag at the 5′-end of one strand and a radiolabel at the 5′-end of another strand, is immobilized on the streptavidin-coated magnetic beads at a low density to prevent formation of synaptic complexes and to report the catalytic activity of enzyme bound to a single DNA site. (B) Addition of non-biotinylated oligonucleotide duplex (activator DNA) into the reaction mixture enables formation of synaptic complexes between the enzyme, the immobilized DNA and the activator DNA in solution. (**C**) Time dependence of the immobilized DNA cleavage. Upon addition of 1000 nM of the wt Ecl18kI (open blue circles) or R174A mutant (open red triangles), cleavage of the immobilized oligoduplex (~1 nM) was monitored by removing samples at timed intervals and analysing them as described in 'Materials and Methods' section. Cleavage of the immobilized substrate was also performed in the presence of 500 nM of non-biotinylated cognate oligoduplex SP25(PTO) (Table 1) (filled blue circles for the wt Ecl18kI and filled red triangles for the R174A mutant). All data points are presented as mean values from three independent experiments ±1 SD.

Table 3. Cognate oligoduplex cleavage by wt Ecl18kI and R174A mutant

Reaction conditions		Rate constants, s^{-1}	
Labelled bio-SP33 substrate (1 nM)	DNA added in solution (500 nM)	Wt Ecl18kI (1000 nM)	R174A mutant (1000 nM)
Immobilized	–	$5.9 \pm 0.8 \times 10^{-4}$	$5.8 \pm 0.6 \times 10^{-4}$
	Cognate SP25 (PTO)	$2.9 \pm 0.1 \times 10^{-2}$	$4.6 \pm 0.2 \times 10^{-4}$
	Non-cognate NSP25	$7.1 \pm 0.9 \times 10^{-4}$	$3.9 \pm 0.2 \times 10^{-4}$
	Precleaved cognate SP25	$4.3 \pm 0.2 \times 10^{-4}$	$4.0 \pm 0.4 \times 10^{-4}$
In solution	Cognate SP25 (PTO)	$4.2 \pm 0.1 \times 10^{-2}$	$4.4 \pm 0.1 \times 10^{-4}$

Both the wt Ecl18kI and the R174A mutant cleave immobilized DNA very slowly (Figure 5C and Table 3). In the presence of the cognate oligoduplex SP25(PTO), the rate of the immobilized DNA cleavage by wt Ecl18kI increases ~50-fold (Figure 5C and Table 3). The non-cognate NSP25 or the precleaved cognate SP25 oligoduplexes (Table 1) show no effect on the cleavage rate (Table 3). Contrary to wt Ecl18kI, the R174A mutant shows no increase in the immobilized DNA cleavage rate in response to the activator DNA and cuts immobilized substrate at low residual rate (Figure 5C and Table 3). Hence, the immobilized DNA cleavage assay indicates that Ecl18kI requires binding of two copies of cognate DNA for optimal catalytic activity. It is likely that the R174A mutation at the Ecl18kI dimer–dimer interface prevents tetramerization upon DNA binding; therefore, the R174A mutant is able to bind only a single DNA molecule and cleave it at a low rate.

Table 4. Cleavage of one- and two-site DNA fragments by wt Ecl18kI and R174A mutant at different ionic strengths

Reaction conditions		Rate constants, s^{-1}	
Ionic strength	DNA substrate (1 nM)	Wt Ecl18kI (2 nM)	R174A mutant (2 nM)
Low (130 mM)	One-site	$8.4 \pm 0.6 \times 10^{-4}$	$4.0 \pm 0.3 \times 10^{-4}$
	Two-site	$7.0 \pm 0.3 \times 10^{-3}$	$4.6 \pm 0.6 \times 10^{-4}$
High (230 mM)	One-site	$2.1 \pm 0.3 \times 10^{-5}$	$1.3 \pm 0.1 \times 10^{-5}$
	Two-site	$2.7 \pm 0.1 \times 10^{-3}$	$1.5 \pm 0.1 \times 10^{-5}$

To find out whether the observed cleavage rates are affected by the substrate immobilization, we measured the cleavage rates in solution under conditions favouring formation of the synaptic complexes. In these experiments, the labelled cognate oligoduplex bio-SP33 and the activator oligoduplex SP25(PTO) were mixed in solution at a 1:500 ratio and Ecl18kI or the R174A mutant were added to the reaction mixture. Under a large excess of the SP25(PTO) oligoduplex, the concentration of the synaptic complexes including two labelled cognate oligoduplexes bio-SP33 is negligible and all labelled DNA molecules are presumably incorporated into mixed synaptic complexes comprised of the cognate bio-SP33 and the activator SP25(PTO) duplexes. Cleavage rate analysis revealed that under these conditions, the wt Ecl18kI cuts cognate oligoduplex 100-fold faster than the R174A mutant, indicating that DNA immobilization on a solid surface does not interfere significantly with DNA cleavage rate (Table 2).

Cleavage of one- and two-site DNA fragments in solution. REases which require binding of two cognate sites for optimal catalytic activity, cleave DNA substrates bearing two targets much more rapidly than a single-site substrate presumably because the synaptic complexes formed between two sites *in cis* are more stable than *in trans* complexes (8–10,49). According to AFM analysis, wt Ecl18kI forms synaptic complexes between two sites located both *in cis* and *in trans* (Figure 3A and Supplementary Figure S2); therefore, we have compared Ecl18kI cleavage rates of the one- and two-site DNA fragments used in the AFM experiments. Cleavage reactions (Table 4) were performed using similar concentrations of DNA (1 nM) and enzyme (2 nM of wt Ecl18kI or R174A mutant) in both low and high salt buffers since ionic

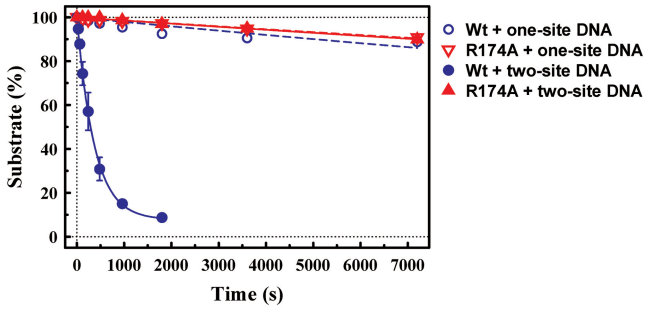

Figure 6. One- and two-site DNA fragment cleavage by Ecl18kI at high ionic strength. The DNA fragments (1 nM) were cleaved using 2 nM wt Ecl18kI (open and filled blue circles) and the R174A mutant (open and filled red triangles) as described in 'Materials and Methods' section. Reaction rate constant values are provided in Table 4.

Table 5. Recognition sequences and functional oligomeric state of evolutionarily related restriction enzymes

Enzyme	Recognition sequence	Oligomeric state
HpyF100III	↓CCGG	n.d.
AgeI	A↓CCGGT	n.d.
Kpn2I	T↓CCGGA	n.d.
NgoMIV	G↓CCGGC	Tetramer
BsaWI	W↓CCGGW	n.d.
Bse634I/Cfr10I	R↓CCGGY	Tetramer
SgrAI	CR↓CCGGYG	Transient tetramer
PspGI	↓CCWGG	Dimer
EcoRII-C	↓CCWGG	Dimer
Ecl18kI	↓CCNGG	Transient tetramer
PfoI	T↓CCNGGA	Dimer n.d.

↓indicates cleavage position. n.d., not determined.

strength may have an effect on cleavage rates due to the different stability of *in cis* and *in trans* synaptic complexes (50). At low salt, the wt Ecl18kI cleaves the two-site fragment ~8-fold faster than the DNA substrate with a single recognition site (Table 4). At high salt, the wt Ecl18kI cuts the two-site substrate ~130-fold faster than the single-site fragment (Figure 6 and Table 4). The R174A mutant under both conditions cuts both DNA fragments with a slow rate similar to that of the wt enzyme on a single-site DNA (Table 4). These data indicate that at increased ionic strength, the wt Ecl18kI tetramer forms stable synaptic complexes between two recognition sites located *in cis* and these are more stable than *in trans* complexes. The ability of the R174A mutant dimer to form transient tetramer and synaptic complexes is impaired; therefore, it cuts both one- and two-site DNA at a slow rate regardless of the buffer ionic strength.

DISCUSSION

Type II restriction enzymes are often arranged as homodimers (e.g. EcoRI or BamHI) or tetramers (e.g. SfiI, NgoMIV). Dimeric REases bind to individual copies of their recognition site, and, if multiple sites are present in DNA molecule, cleave each site in a separate reaction. In contrast, a REase tetramer has two DNA binding interfaces and can form a synaptic complex bridging two recognition sites. After formation of the synaptic complex, tetrameric REases cut both DNA strands at both copies of the recognition site. Furthermore, tetrameric REases show their maximal activity while interacting with two target sites but are virtually inactive (or show only low residual cleavage) on a single recognition site.

SfiI tetramer synapses recognition sites through the loop capture

Bridging of two recognition sites located in the same DNA molecule, loops out an intervening DNA segment. DNA looping by the tetrameric SfiI REase has been demonstrated both by biochemical methods and AFM (37,42). In the presence of Ca^{2+}, wt SfiI binds to its target recognition sites forming stable loops (37,39). To study looping dynamics, the catalytically inactive D79A mutant, which showed rapid association/dissociation kinetics with the recognition sequence has been used (51). The interaction dynamics between the SfiI mutant and DNA was followed in real time by the TPM method (39). TPM experiments allowed determination of the SfiI tetramer association and dissociation rates with a single recognition site and the dynamics of subsequent loop formation and breakage. SfiI dissociation/association, loop formation, loop breakage and DNA (bead) release rates obtained in single molecule experiments were in the close agreement with bulk rates determined in biochemical experiments (39,51). Other tetrameric restriction enzymes such as Cfr10I, Bse634I and NgoMIV (9,10,12) presumably follow a similar mechanism. Surprisingly, the SgrAI which is evolutionarily related to the tetrameric REases (Table 5) and which was expected to be a tetramer, follows a distinct reaction pathway. SgrAI is a dimer in free solution (19) and shows a dimer bound to a single DNA copy in the crystal (52). However, according to biochemical data, it displays its maximal activity on DNA with two copies of its recognition sequence and bridges two recognition sites in the 3D process. It is thought that two DNA-bound SgrAI dimers may associate into a tetramer that has enhanced activity, which then concurrently cleaves both sites. The quantitative details of the SgrAI reaction pathway, however, are not yet available.

Ecl18kI synapses two recognition sites through the protein–protein association

Similar to SgrAI, the Ecl18kI enzyme exists as a dimer in solution (28) but in the crystal structure it shows a tetramer bound to two DNA molecules (22) (Figure 1). To determine the reaction pathway followed by Ecl18kI, we have analysed Ecl18kI interactions with DNA containing and one or two recognition sites. AFM experiments on the two-site DNA fragment demonstrate that Ecl18I synapses two recognition sites looping out intervening DNA (Figure 3). In the case of a single-site DNA, X-like *trans*-synaptic complexes are observed. Protein volume measurements indicate that in the synaptic complexes Ecl18kI is arranged as a tetramer. A smaller

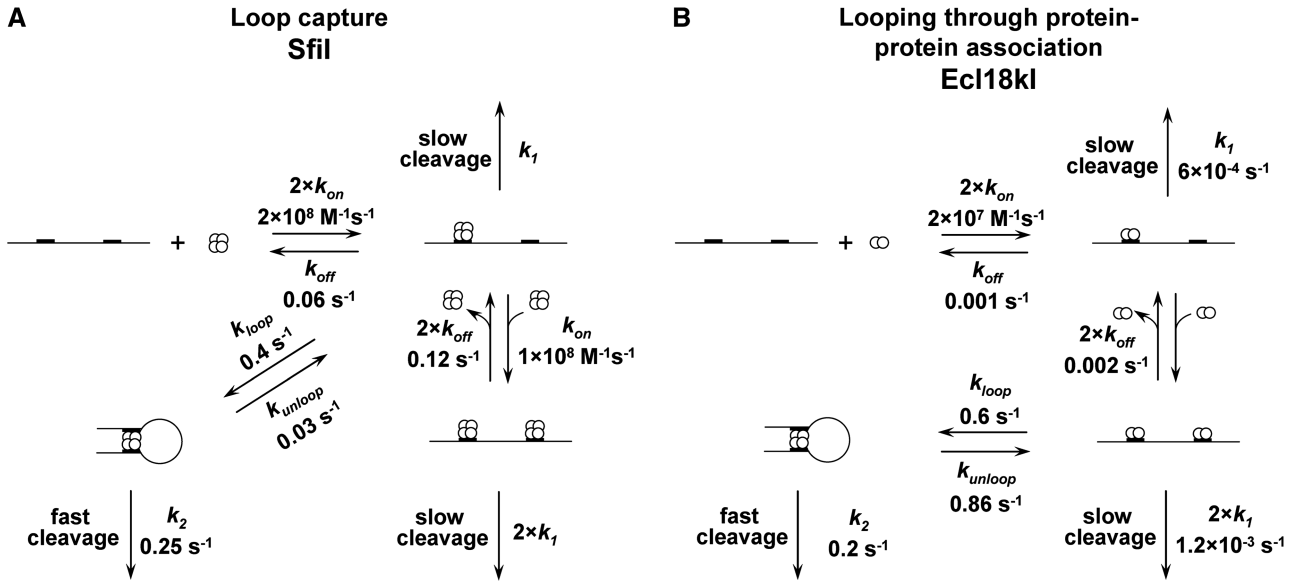

Figure 7. REases SfiI and Ecl18kI on the two-site DNA. Cartoons depict the schematic mechanism of the two-site DNA cleavage by SfiI (**A**) and Ecl18kI (**B**). In the case of SfiI (**A**), a single DNA-bound tetramer may either slowly cleave the individual DNA site (rate constant k_1), or capture the second unoccupied site looping out the intervening DNA to form the catalytically competent synaptic complex which is rapidly resolved into the final reaction products (rate constant k_2). Binding of the second tetramer at increased SfiI concentrations produces an unlooped protein-DNA complex, where two tetramers act independently on two DNA sites and slowly cleave DNA ($2 \times k_1$). (**B**) At Ecl18kI concentrations much below that of the DNA, a single Ecl18kI dimer presumably binds to only one individual target site, resulting in slow DNA cleavage (rate constant k_1). Binding of the second dimer at increased enzyme concentrations produces an unlooped protein-DNA complex, where two dimers act on the two DNA sites independently ($2 \times k_1$). Tetramerization of two DNA-bound Ecl18kI dimers results in the looped synaptic complex, which is optimal for catalysis and results in fast cleavage (rate constant k_2). The k_{on}, k_{off}, force corrected k_{loop} and k_{unloop} values for SfiI and Ecl18kI were extracted from the TPM experiments (39). The k_1 and k_2 values for Ecl18kI were calculated from immobilized oligoduplex cleavage data (this work), and solution experiments under optimal cleavage conditions (53), respectively. The k_2 value for SfiI was extracted from the TPM experiments (39).

fraction of DNA molecules are linear and contain the Ecl18kI dimer bound to the single recognition site (images not shown). Thus, Ecl18kI binds to the target site presumably as a dimer and two Ecl18kI dimers associate into a tetramer looping out intervening DNA. The TPM data supports this model and demonstrates that DNA looping by Ecl18kI is a highly dynamic process. The thresholded trace (Figure 4A, left panel, red line) shows that the looping comes in bursts: once two Ecl18kI dimers are bound to the DNA, the tether shows dynamic looping, spending only a short time in the unlooped state. As soon as one (or both) of the dimers detaches from the recognition site, significantly longer pauses are observed. A similar associative model has also been proposed for the formation of the RAG1/RAG2 synaptic complex (44).

DNA cleavage studies show that the Ecl18kI synaptic complex is required for catalysis. Indeed, Ecl18kI slowly cuts single-site DNA immobilized on the surface at low density, but cleavage is stimulated by a second cognate DNA copy provided *in trans* (Figure 5 and Table 3). In solution, under conditions favouring *cis*-synaptic complex formation, Ecl18kI cuts DNA fragments containing two recognition sites much faster than a single-site DNA. Thus, the available data indicate that Ecl18kI in solution makes a catalytically competent synaptic complex bridging two DNA copies. Therefore, the crystal structure of Ecl18kI showing two DNA molecules bound by the tetramer (Figure 1) is of the X-like *trans*-synaptic complex. Mutational analysis of the amino acid residues located at the Ecl18kI dimer–dimer interface supports the importance of tetramerization in the function of Ecl18kI. Indeed, in the case of the R174A mutant, only ~3% of protein–DNA complexes display loops and no specific looping events are detected in the TPM experiments. Protein volume analysis in the AFM experiments indicates that the R174A mutant is bound to DNA as a dimer. Furthermore, the R174A mutant under all experimental conditions tested cleaves immobilized DNA at a low rate similar to that of the wt Ecl18kI interacting with a single target site (Figure 5 and Table 3). In summary, the available data indicate that the R174A mutation interferes with tetramer assembly and formation of the catalytically competent synaptic complex.

Reaction pathway of Ecl18kI

Taken together, the experimental data obtained in this study are consistent with the following reaction scheme (Figure 7B). At protein concentrations much below that of the DNA, the Ecl18kI dimer presumably binds to one of the two target sites ($k_{on} = 1 \times 10^7\,M^{-1}\,s^{-1}$) yielding an Ecl18kI dimer–DNA complex ($k_{off} = 0.001\,s^{-1}$) which shows only slow cleavage ($k_1 = 6 \times 10^{-4}\,s^{-1}$). Binding of the second enzyme dimer at increased protein concentrations produces an unlooped protein-DNA complex, where each Ecl18kI dimer is bound to the individual site and acts independently slowly cleaving DNA ($2 \times k_1 = 1.2 \times 10^{-3}\,s^{-1}$). Association of the two

DNA-bound dimers ($k_{loop} = 0.6\,s^{-1}$) yields a looped synaptic complex, which is optimal for catalysis and results in fast DNA cleavage ($k_2 = 0.2\,s^{-1}$). Under these conditions Ecl18kI cleavage rate is ~200-fold faster in comparison with the Ecl18kI dimer acting on the single site. DNA looping by the wt Ecl18kI is a highly dynamic process. The oscillation between the looped and unlooped states is fast with a lifetime of the looped complex of ~1 s. In contrast to Ecl18kI, the R174A mutant of Ecl18kI binds DNA as a dimer but is unable to form looped protein-DNA complexes and therefore cleaves DNA slowly.

The variety of the mechanisms employed by restriction enzymes to achieve DNA cleavage continues to surprise. Ecl18kI recognizes the 5′-CCNGG-3′ sequence and belongs to a large group of evolutionarily related REases, which recognize target sites containing 5′-CCGG-3′ or 5′-CCNGG-3′ nucleotides embedded within different flanking sequences (Table 5). The enzymes that belong to this group show diverse oligomeric structures and mechanisms. EcoRII-C and PspGI are functional as homodimers, which interact with a single DNA copy, while NgoMIV, Cfr10I and Bse634I are arranged as stable tetramers and interact with two DNA copies presumably capturing two target sites into a synaptic complex (Figure 7A). Ecl18kI, like SgrAI, employs a different mechanism (Figure 7B). Ecl18kI is a dimer in solution but forms a transient, catalytically competent synaptic complex through the association of the two DNA-bound dimers. In conclusion, our studies demonstrate that these related enzymes have developed diverse mechanistic strategies to ensure a tight coupling between target site recognition and cleavage.

SUPPLEMENTARY DATA

Supplementary Data are available at NAR Online.

FUNDING

Lithuania State Science and Studies Foundation (grants T-14/07, T-27/08 to M.Z., G.T. and V.S.); FP6 Marie Curie network 'DNA enzymes' (to A.O.); LASERLAB EUROPE Access to research infrastructures grant (to V.S. and G.J.L.W.); grants from National Institutes of Health (GM062235 to Y.L.L.); Nebraska Research Initiative (NRI) (to Y.L.L.); Fundamenteel Onderzoek der Materie (FOM) research program 'Physics of the Genome', financially supported by 'Nederlandse Organisatie voor Wetenschappelijk Onderzoek (NWO)' (to N.L. and G.J.L.W) and VICI grant of NWO (to G.J.L.W.). Funding for open access charge: FP6 Marie Curie network 'DNA enzymes' and FP7 Grant 'MoBiLi' (245721).

Conflict of interest statement. None declared.

REFERENCES

1. Pingoud,A., Fuxreiter,M., Pingoud,V. and Wende,W. (2005) Type II restriction endonucleases: structure and mechanism. *Cell Mol. Life Sci.*, **62**, 685–707.
2. Orlowski,J. and Bujnicki,J.M. (2008) Structural and evolutionary classification of Type II restriction enzymes based on theoretical and experimental analyses. *Nucleic Acids Res.*, **36**, 3552–3569.
3. Sokolowska,M., Kaus-Drobek,M., Czapinska,H., Tamulaitis,G., Szczepanowski,R.H., Urbanke,C., Siksnys,V. and Bochtler,M. (2007) Monomeric restriction endonuclease BcnI in the apo form and in an asymmetric complex with target DNA. *J. Mol. Biol.*, **369**, 722–734.
4. Kaus-Drobek,M., Czapinska,H., Sokolowska,M., Tamulaitis,G., Szczepanowski,R.H., Urbanke,C., Siksnys,V. and Bochtler,M. (2007) Restriction endonuclease MvaI is a monomer that recognizes its target sequence asymmetrically. *Nucleic Acids Res.*, **35**, 2035–2046.
5. Sasnauskas,G., Halford,S.E. and Siksnys,V. (2003) How the BfiI restriction enzyme uses one active site to cut two DNA strands. *Proc. Natl Acad. Sci. USA*, **100**, 6410–6415.
6. Pingoud,A. and Jeltsch,A. (2001) Structure and function of type II restriction endonucleases. *Nucleic Acids Res.*, **29**, 3705–3727.
7. Siksnys,V., Grazulis,S. and Huber,R. (2004) Structure and function of the tetrameric restriction enzymes. In Pingoud,A. (ed.), *Restriction Endonucleases*, Vol. 14. Springer, Berlin, pp. 237–259.
8. Wentzell,L.M., Nobbs,T.J. and Halford,S.E. (1995) The SfiI restriction endonuclease makes a four-strand DNA break at two copies of its recognition sequence. *J. Mol. Biol.*, **248**, 581–595.
9. Deibert,M., Grazulis,S., Sasnauskas,G., Siksnys,V. and Huber,R. (2000) Structure of the tetrameric restriction endonuclease NgoMIV in complex with cleaved DNA. *Nat. Struct. Biol.*, **7**, 792–799.
10. Siksnys,V., Skirgaila,R., Sasnauskas,G., Urbanke,C., Cherny,D., Grazulis,S. and Huber,R. (1999) The Cfr10I restriction enzyme is functional as a tetramer. *J. Mol. Biol.*, **291**, 1105–1118.
11. Grazulis,S., Deibert,M., Rimseliene,R., Skirgaila,R., Sasnauskas,G., Lagunavicius,A., Repin,V., Urbanke,C., Huber,R. and Siksnys,V. (2002) Crystal structure of the Bse634I restriction endonuclease: comparison of two enzymes recognizing the same DNA sequence. *Nucleic Acids Res.*, **30**, 876–885.
12. Zaremba,M., Sasnauskas,G., Urbanke,C. and Siksnys,V. (2005) Conversion of the tetrameric restriction endonuclease Bse634I into a dimer: oligomeric structure-stability-function correlations. *J. Mol. Biol.*, **348**, 459–478.
13. Bellamy,S.R., Milsom,S.E., Kovacheva,Y.S., Sessions,R.B. and Halford,S.E. (2007) A switch in the mechanism of communication between the two DNA-binding sites in the SfiI restriction endonuclease. *J. Mol. Biol.*, **373**, 1169–1183.
14. Bellamy,S.R., Mina,P., Retter,S.E. and Halford,S.E. (2008) Fidelity of DNA sequence recognition by the SfiI restriction endonuclease is determined by communications between its two DNA-binding sites. *J. Mol. Biol.*, **384**, 557–563.
15. Bitinaite,J., Wah,D.A., Aggarwal,A.K. and Schildkraut,I. (1998) FokI dimerization is required for DNA cleavage. *Proc. Natl Acad. Sci. USA*, **95**, 10570–10575.
16. Sanders,K.L., Catto,L.E., Bellamy,S.R. and Halford,S.E. (2009) Targeting individual subunits of the FokI restriction endonuclease to specific DNA strands. *Nucleic Acids Res.*, **37**, 2105–2115.
17. Ibryashkina,E.M., Sasnauskas,G., Solonin,A.S., Zakharova,M.V. and Siksnys,V. (2009) Oligomeric structure diversity within the GIY-YIG nuclease family. *J. Mol. Biol.*, **387**, 10–16.
18. Gasiunas,G., Sasnauskas,G., Tamulaitis,G., Urbanke,C., Razaniene,D. and Siksnys,V. (2008) Tetrameric restriction enzymes: expansion to the GIY-YIG nuclease family. *Nucleic Acids Res.*, **36**, 938–949.
19. Daniels,L.E., Wood,K.M., Scott,D.J. and Halford,S.E. (2003) Subunit assembly for DNA cleavage by restriction endonuclease SgrAI. *J. Mol. Biol.*, **327**, 579–591.
20. Wood,K.M., Daniels,L.E. and Halford,S.E. (2005) Long-range communications between DNA sites by the dimeric restriction endonuclease SgrAI. *J. Mol. Biol.*, **350**, 240–253.
21. Den'mukhametov,M.M., Zakharova,M.V., Kravets,A.N., Pertsev,A.V., Sineva,E.V., Repik,A.V., Beletskaia,I.V., Gromova,E.S. and Solonin,A.S. (1997) Characteristics of a plasmid bearing a gene of a restriction modification type II system–the SsoII isoschizomer. *Mol. Biol.*, **31**, 831–838.

22. Bochtler,M., Szczepanowski,R.H., Tamulaitis,G., Grazulis,S., Czapinska,H., Manakova,E. and Siksnys,V. (2006) Nucleotide flips determine the specificity of the Ecl18kI restriction endonuclease. *EMBO J.*, **25**, 2219–2229.
23. Szczepanowski,R.H., Carpenter,M.A., Czapinska,H., Zaremba,M., Tamulaitis,G., Siksnys,V., Bhagwat,A.S. and Bochtler,M. (2008) Central base pair flipping and discrimination by PspGI. *Nucleic Acids Res.*, **36**, 6109–6117.
24. Golovenko,D., Manakova,E., Tamulaitiene,G., Grazulis,S. and Siksnys,V. (2009) Structural mechanisms for the 5′-CCWGG sequence recognition by the N- and C-terminal domains of EcoRII. *Nucleic Acids Res.*, **37**, 6613–6624.
25. Reuter,M., Kupper,D., Meisel,A., Schroeder,C. and Kruger,D.H. (1998) Cooperative binding properties of restriction endonuclease EcoRII with DNA recognition sites. *J. Biol. Chem.*, **273**, 8294–8300.
26. Pingoud,V., Conzelmann,C., Kinzebach,S., Sudina,A., Metelev,V., Kubareva,E., Bujnicki,J.M., Lurz,R., Luder,G., Xu,S.Y. *et al.* (2003) PspGI, a type II restriction endonuclease from the extreme thermophile Pyrococcus sp.: structural and functional studies to investigate an evolutionary relationship with several mesophilic restriction enzymes. *J. Mol. Biol.*, **329**, 913–929.
27. Tamulaitis,G., Mucke,M. and Siksnys,V. (2006) Biochemical and mutational analysis of EcoRII functional domains reveals evolutionary links between restriction enzymes. *FEBS Lett.*, **580**, 1665–1671.
28. Tamulaitis,G., Solonin,A.S. and Siksnys,V. (2002) Alternative arrangements of catalytic residues at the active sites of restriction enzymes. *FEBS Lett.*, **518**, 17–22.
29. Shlyakhtenko,L.S., Gilmore,J., Portillo,A., Tamulaitis,G., Siksnys,V. and Lyubchenko,Y.L. (2007) Direct visualization of the EcoRII-DNA triple synaptic complex by atomic force microscopy. *Biochemistry*, **46**, 11128–11136.
30. Lyubchenko,Y.L. and Shlyakhtenko,L.S. (2009) AFM for analysis of structure and dynamics of DNA and protein-DNA complexes. *Methods*, **47**, 206–213.
31. Lyubchenko,Y.L., Shlyakhtenko,L.S. and Gall,A.A. (2009) Atomic force microscopy imaging and probing of DNA, proteins, and protein DNA complexes: silatrane surface chemistry. *Methods Mol. Biol.*, **543**, 337–351.
32. Tamulaitis,G., Sasnauskas,G., Mucke,M. and Siksnys,V. (2006) Simultaneous binding of three recognition sites is necessary for a concerted plasmid DNA cleavage by EcoRII restriction endonuclease. *J. Mol. Biol.*, **358**, 406–419.
33. Tamulaitis,G., Zaremba,M., Szczepanowski,R.H., Bochtler,M. and Siksnys,V. (2007) Nucleotide flipping by restriction enzymes analyzed by 2-aminopurine steady-state fluorescence. *Nucleic Acids Res.*, **35**, 4792–4799.
34. Shlyakhtenko,L.S., Gall,A.A., Filonov,A., Cerovac,Z., Lushnikov,A. and Lyubchenko,Y.L. (2003) Silatrane-based surface chemistry for immobilization of DNA, protein-DNA complexes and other biological materials. *Ultramicroscopy*, **97**, 279–287.
35. Lyubchenko,Y.L. and Shlyakhtenko,L.S. (2009) AFM for analysis of structure and dynamics of DNA and protein-DNA complexes. *Methods*, **47**, 206–213.
36. Lyubchenko,Y.L., Gall,A.A. and Shlyakhtenko,L.S. (2001) Atomic force microscopy of DNA and protein-DNA complexes using functionalized mica substrates. *Methods Mol. Biol.*, **148**, 569–578.
37. Lushnikov,A.Y., Potaman,V.N., Oussatcheva,E.A., Sinden,R.R. and Lyubchenko,Y.L. (2006) DNA strand arrangement within the SfiI-DNA complex: atomic force microscopy analysis. *Biochemistry*, **45**, 152–158.
38. Shlyakhtenko,L.S., Lushnikov,A.Y. and Lyubchenko,Y.L. (2009) Dynamics of nucleosomes revealed by time-lapse atomic force microscopy. *Biochemistry*, **48**, 7842–7848.
39. Laurens,N., Bellamy,S.R., Harms,A.F., Kovacheva,Y.S., Halford,S.E. and Wuite,G.J. (2009) Dissecting protein-induced DNA looping dynamics in real time. *Nucleic Acids Res.*, **37**, 5454–5464.
40. Colquhoun,D. and Sigworth,F.J. (1983) Fitting and statistical analysis of single-channel records. In Sakmann,B. and Neher,E. (eds), *Single channel recording*. Plenum Press, New York and London, pp. 191–263.
41. Yoshioka,K. (2002) KyPlot – a user-oriented tool for statistical data analysis and visualization. *CompStat.*, **17**, 425–437.
42. Watson,M.A., Gowers,D.M. and Halford,S.E. (2000) Alternative geometries of DNA looping: an analysis using the SfiI endonuclease. *J. Mol. Biol.*, **298**, 461–475.
43. Gilmore,J.L., Suzuki,Y., Tamulaitis,G., Siksnys,V., Takeyasu,K. and Lyubchenko,Y.L. (2009) Single-molecule dynamics of the DNA-EcoRII protein complexes revealed with high-speed atomic force microscopy. *Biochemistry*, **48**, 10492–10498.
44. Shlyakhtenko,L.S., Gilmore,J., Kriatchko,A.N., Kumar,S., Swanson,P.C. and Lyubchenko,Y.L. (2009) Molecular mechanism underlying RAG1/RAG2 synaptic complex formation. *J. Biol. Chem.*, **284**, 20956–20965.
45. van den Broek,B., Vanzi,F., Normanno,D., Pavone,F.S. and Wuite,G.J. (2006) Real–time observation of DNA looping dynamics of Type IIE restriction enzymes NaeI and NarI. *Nucleic Acids Res.*, **34**, 167–174.
46. Segall,D.E., Nelson,P.C. and Phillips,R. (2006) Volume-exclusion effects in tethered-particle experiments: bead size matters. *Phys. Rev. Lett.*, **96**, 088306.
47. Embleton,M.L., Siksnys,V. and Halford,S.E. (2001) DNA cleavage reactions by type II restriction enzymes that require two copies of their recognition sites. *J. Mol. Biol.*, **311**, 503–514.
48. Zaremba,M., Sasnauskas,G., Urbanke,C. and Siksnys,V. (2006) Allosteric communication network in the tetrameric restriction endonuclease Bse634I. *J. Mol. Biol.*, **363**, 800–812.
49. Lagunavicius,A., Sasnauskas,G., Halford,S.E. and Siksnys,V. (2003) The metal-independent type IIs restriction enzyme BfiI is a dimer that binds two DNA sites but has only one catalytic centre. *J. Mol. Biol.*, **326**, 1051–1064.
50. Nobbs,T.J. and Halford,S.E. (1995) DNA cleavage at two recognition sites by the SfiI restriction endonuclease: salt dependence of cis and trans interactions between distant DNA sites. *J. Mol. Biol.*, **252**, 399–411.
51. Bellamy,S.R., Kovacheva,Y.S., Zulkipli,I.H. and Halford,S.E. (2009) Differences between Ca2+ and Mg2+ in DNA binding and release by the SfiI restriction endonuclease: implications for DNA looping. *Nucleic Acids Res.*, **37**, 5443–5453.
52. Dunten,P.W., Little,E.J., Gregory,M.T., Manohar,V.M., Dalton,M., Hough,D., Bitinaite,J. and Horton,N.C. (2008) The structure of SgrAI bound to DNA; recognition of an 8 base pair target. *Nucleic Acids Res.*, **36**, 5405–5416.
53. Tamulaitis,G., Zaremba,M., Szczepanowski,R.H., Bochtler,M. and Siksnys,V. (2008) How PspGI, catalytic domain of EcoRII and Ecl18kI acquire specificities for different DNA targets. *Nucleic Acids Res.*, **36**, 6101–6108.